Single-pass forming for three-dimensional microstructures by high-speed shearing of multilayer thin films

Tetsuya Hamaguchi and Hiroki Yonemoto
Department of Engineering Synthesis, Graduate School of Engineering, The University of Tokyo, 7-3-1 Hongo, Bunkyo-ku, Tokyo 113-8656, Japan

Keisuke Nagato[a)]
Department of Engineering Synthesis, Graduate School of Engineering, The University of Tokyo, 7-3-1 Hongo, Bunkyo-ku, Tokyo 113-8656, Japan and Research Fellow of the Japan Society for the Promotion of Science, 8 Ichibancho, Chiyoda-ku, Tokyo 102-8472, Japan

Kensuke Tsuchiya
Institute of Industrial Science, The University of Tokyo, 4-6-1 Komaba, Meguro-ku, Tokyo 153-8505, Japan

Masayuki Nakao
Department of Engineering Synthesis, Graduate School of Engineering, The University of Tokyo, 7-3-1 Hongo, Bunkyo-ku, Tokyo 113-8656, Japan

(Received 25 April 2008; accepted 25 August 2008; published 25 September 2008)

The authors propose a single-pass forming technique for three-dimensional microstructures by shearing multilayer thin films. At a high strain rate, when strain is applied to a material at a speed higher than that of plastic wave propagation, the material is generally fractured without plastic deformation. In their experiment, a punch freely falling onto the back of a microfabricated mold allowed a high strain rate to be applied to the substrate. Multilayer thin films of eight evaporated layers of 250-nm-thick Si and SiO were successfully deformed to the bottom layer when the strain rate was over 1000–1500 s^{-1}. © *2008 American Vacuum Society.* [DOI: 10.1116/1.2982241]

I. INTRODUCTION

Three-dimensional (3D) microstructures built in microelectromechanical-system (MEMS) or chip-based optical devices[1–3] have generated great interest. These devices are commonly fabricated by using very large-scale integration or MEMS processes such as thin-film deposition, high-resolution lithography, and deep etching. However, 3D microstructures cannot be fabricated at low cost using these two-dimensional processes.

In particular, 3D photonic crystals, in which light-wavelength-scale materials with alternating different refractive indexes are periodically ordered in 3D, promise optical devices such as photonic guides or high-efficiency filters due to their fine photonic bandgaps.[4] To date, piling techniques of multilayered nanostructure[5–9] and self-crowning techniques[10,11] have been proposed to fabricate 3D photonic crystals. In the piling-up methods, straight bars are micromachined in lines on a substrate's face, and they are piled up and bonded repeatedly. For self-crowned crystals, high-refractive-index thin films and low-refractive-index thin films are alternately sputtered with bias power on a basic nanostructured substrate. In contrast, we propose a new fabrication method that shears multilayer thin films and shifts them together in a single pass (Fig. 1). A microfabricated mold presses preliminarily formed thin films with different refractive indexes. High-speed pressing produces a high strain rate on the materials and realizes vertical shearing

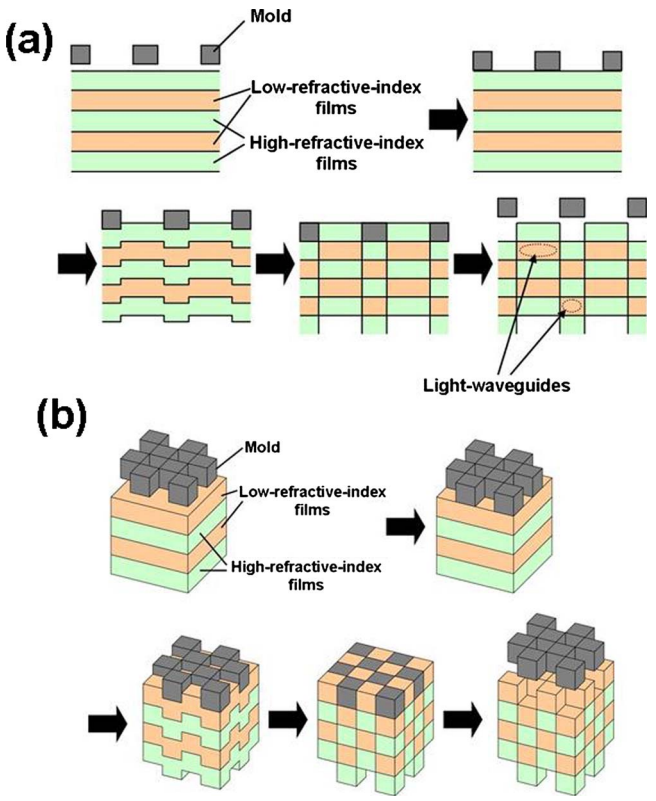

FIG. 1. Schematic of single-pass forming of (a) chip-based light waveguides and (b) 3D periodic microstructures using high-speed shearing of multilayer thin films.

a)Author to whom correspondence should be addressed; Tel.: +81-3-5841-6362; electronic mail: nagato@hnl.t.u-tokyo.ac.jp.

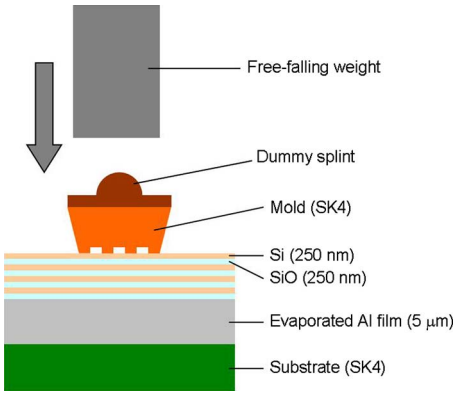

FIG. 2. Schematic of experimental setup for testing high-speed shearing of multilayer thin films.

because of the limitation of the speed of deformation-wave propagation. By using the mold to shift the multilayer thin film by a length corresponding to the thickness of a single layer of the multilayer film, low-refractive-index waveguides can be surrounded by high-refractive-index materials [Fig. 1(a)] or cubes with different refractive indexes alternately ordered three dimensionally [Fig. 1(b)]. The greatest advantage of this method is that we do not need to position each layer of the multilayer film. This single-pass replication method leads to the high-throughput and low-cost fabrication of 3D microstructures. In this study, we investigate the shearing effect as a function of strain rate using a microfabricated mold and Si/SiO evaporated thin films.

II. EXPERIMENTAL METHODS

In general shearing processes (e.g., punching), an upper mold and an under mold are used. However, positioning the two molds on the nanometer scale is difficult due to thermal deformation of the equipment. We suggest a method without an under mold, as shown in Fig. 2. A cushion layer under multilayer thin films was sacrificially deformed. In this study, a thick Al film (5 μm) was evaporated as a cushioning layer on a polished substrate (SK4, alloy tool steel, JIS, $H_{RC} > 64$) before forming the multilayer thin films. Four sets of Si/SiO layers were evaporated to 250 nm thicknesses. A checker-patterned mold was fabricated with a focused ion beam (FIB) (FB-2000A: Hitachi) on an SK4 substrate of 5 μm wide and 200–300 nm deep in an area of 1 mm. Figure 3 shows a scanning electron microscopy (SEM) (S-4160s: Hitachi) image of the mold. The bottom layers were not finished flat because SK4 is a polycrystalline material and the etching rate was not uniform.

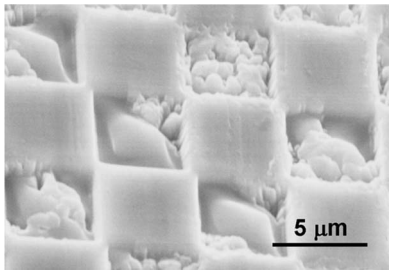

FIG. 3. SEM image of checker-patterned mold fabricated by FIB (tilt angle: 40°).

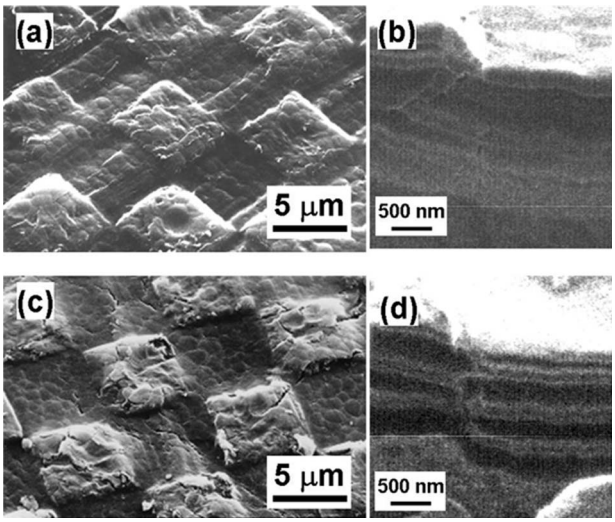

FIG. 4. (a) SEM surface image (tilt angle: 40°), (b) SIM cross-sectional image (tilt angle: 60°) of sample pressed statically (mass of weight: 4.3 kg), (c) SEM surface image, and (d) SIM cross-sectional image of sample pressed at high strain rate (mass of weight: 75 g, strain rate:1500 s^{-1}).

In Fig. 2, a dummy splint (a quenched steel ball 5 mm in diameter) was placed at the back of the mold to prevent the weight from hitting the edges of the mold. The free-falling weight (25 g, 75 g, and 4.3 kg) hits the dummy splint, and as a result, the mold presses the multilayer thin films. The strain rates were calculated from the pressing strokes and the pressing times. The pressing strokes were obtained from scanning ion microscopy (SIM) images of the cross section of shifted thin films. The pressing times were obtained by monitoring the electric conducting state of the free-falling weight and the dummy splint. In this study, we assumed that the conducting time corresponds to the contact time and the pressing time. We controlled the strain rate by varying the speed of the free-falling weight immediately before impact. The cross sections of the multilayer films were formed by FIB, and then SIM images were obtained from the differences in the secondary-electron intensities of Al, Si, and SiO. Note that the SIM observation is a destructive imaging process.

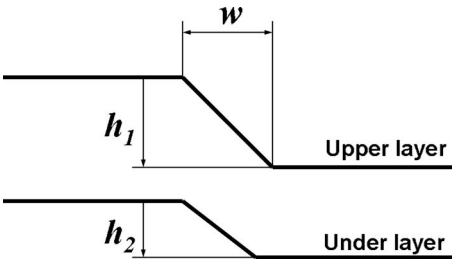

FIG. 5. Deformation model for determining strain.

TABLE I. Deformation conditions and replication factors.

Sample	Mass of weight (g)	ε_1	ε_2	t (ms)	$\dot{\varepsilon}$ (s^{-1})	Replication factor
A	4300	0.92	0.22	10 000	>0.1	0.24
B	75	0.46	0.10	17	270	0.21
C	75	0.53	0.22	7.5	710	0.42
D	75	0.95	0.60	7.5	1270	0.64
E	75	1.10	1.05	7.5	1470	0.95
F	75	1.17	1.10	6.0	1950	0.94

III. RESULTS

A. Shearing effect of static load and impact load

We pressed the multilayer thin films with both a static load and an impact load. First, a weight of 4.3 kg was pressed statically for 10 s. Figure 4 shows a (a) SEM image of the surface and (b) SIM image of a cross section obtained by FIB. Next, a weight of 75 g pressed the multilayer films at high strain rate. Figures 4(c) and 4(d) show a SEM image of the surface and an SIM image of a cross section, respectively. Relatively dark layers are Si, bright layers show SiO, and the bright lowest layer is Al. The surface structures are similar but the internal film layers are deformed differently. To compare the effect of replication, we determined the strain using the shifted strokes of the upper layer (h_1) and the under layer (h_2) and the width of the deformed slope of the surface (w) (Fig. 5). The strains of the upper and under layers are $\varepsilon_1=h_1/w$ and $\varepsilon_2=h_2/w$, respectively. Defining the deformation time as t, we determined the strain rate of the sample ε_1/t in this study. Since the measured contact time on the sample was 7.5 ms, the strain rate of the impact load was calculated to be 1500 s^{-1}. Furthermore, we determined the replication factor $\varepsilon_2/\varepsilon_1$. In this case, the replication factor of the static pressing was 0.24 and that of the impact pressing was 0.95.

B. Effect of strain rate on replication factor

We investigated the effect of strain rate on replication factor. Table I shows deformation conditions and resulting replication factors using a weight of 75 g, together with those of the results in Sec. III A. Figure 6 shows the SIM images of the cross sections. The replication factor of sample B (strain rate: 270 s^{-1}) was similar to that of sample A (static strain). However, higher strain rate resulted in a higher replication factor. The strains in the upper and the under layers were higher with higher strain rate because the higher speed of the free-falling punch caused a higher strain rate; thus, the momentum on the multilayer films increased. Samples E and F with strain rates of 1470 and 1950 s^{-1}, respectively, showed similar results. However, sample F was shifted about 500 nm, which corresponds to the thickness of two layers.

Figure 7 shows the replication factors as a function of strain rate. The replication factor dramatically increases when the strain rates were between 1000 and 1500 s^{-1}. The weight of the free-falling punch did not affect the tendency of changes in the strain rate.

IV. DISCUSSION

In this study, the prototype mold was fabricated using a FIB and the fabrication accuracy was limited. This is because in each cross section, sheared multilayer films have slopes with about 200 nm width, which is comparable to the thickness of one layer of the multilayer films. The bottom surface of the mold was rough. Moreover, the pitch in the area direction was 10 μm, but that in the film-thickness direction was 500 nm; thus, the resultant films do not have good optical properties. We must resolve these issues to fabricate finer mosaic-type 3D photonic crystals, as shown in Fig. 1(b).

V. CONCLUSIONS

We proposed a new method of a single-pass shearing process on multilayer thin films to fabricate 3D photonic crystals. We investigated the effect of strain rate on the replica-

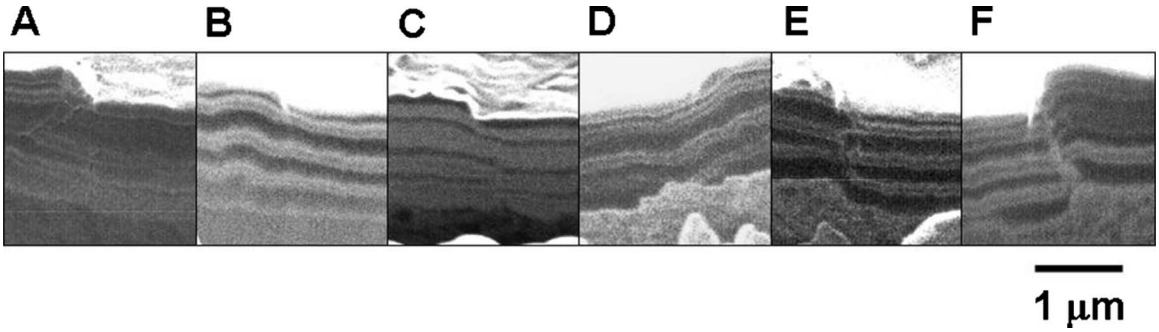

FIG. 6. SIM images of cross sections of deformed layer under conditions listed in Table I (A–F). Tilt angle: 60°.

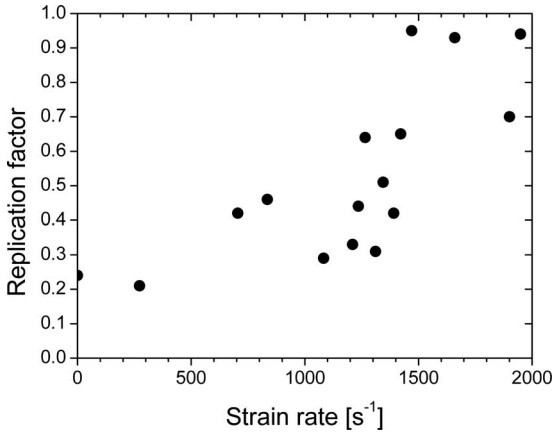

FIG. 7. Replication factor as a function of strain rate.

tion factor using alternating layers of eight evaporated Si/SiO thin films and a cushion layer of an evaporated thick Al film. A free-falling punch produced a high strain rate up to 2000 s^{-1}. The films were sheared well at high strain rates of 1000–1500 s^{-1}. This method will lead to high throughput, low cost, high precision, and high reproducibility fabrication of 3D photonic crystals.

[1]V. R. Almeida, C. A. Barrios, R. R. Panepucci, and M. Lipson, Nature (London) **431**, 1081 (2004).
[2]M. C. Wu, O. Solgaard, and J. E. Ford, J. Lightwave Technol. **24**, 4433 (2006).
[3]J. T. Kim and C.-G. Choi, Sens. Actuators, A **126**, 425 (2006).
[4]E. Yablonovitch, Phys. Rev. Lett. **58**, 2059 (1987).
[5]S. Y. Lin *et al.*, Nature (London) **394**, 251 (1998).
[6]S. Noda, N. Yamamoto, and A. Sasaki, Jpn. J. Appl. Phys., Part 2 **35**, L909 (1996).
[7]S. Noda, K. Tomoda, N. Yamamoto, and A. Chutinan, Science **289**, 604 (2000).
[8]L.-R. Bao, X. Cheng, X. D. Huang, L. J. Guo, S. W. Pang, and A. F. Yee, J. Vac. Sci. Technol. B **20**, 2881 (2002).
[9]M. Nakajima, T. Yoshikawa, K. Sogo, and Y. Hirai, Microelectron. Eng. **83**, 876 (2006).
[10]S. Kawakami, Electron. Lett. **33**, 1260 (1997).
[11]S. Kawakami, T. Kawashima, and T. Sato, Appl. Phys. Lett. **74**, 463 (1999).